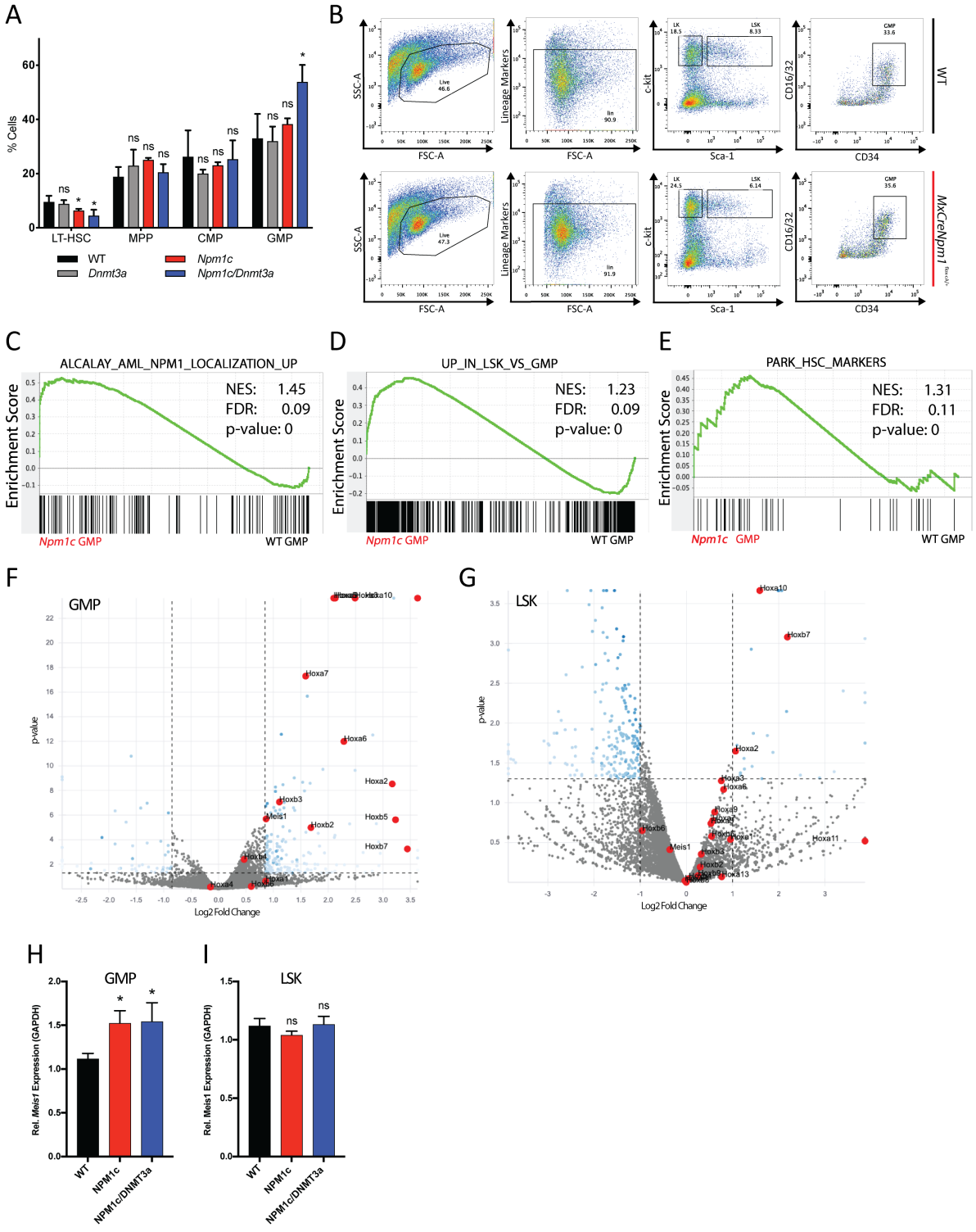

Fig. S1. *Npm1c* is sufficient to induce stem cell gene expression program in myeloid progenitor cells.

(A) FACS analysis of LT-HSC, MPP, CMP and GMP percentages in WT, *MxCreDnmt3a*$^{R878H/+}$, *MxCreNpm1*$^{flox\text{-}cA/+}$ single, and *MxCreNpm1*$^{flox\text{-}cA/+}$*Dnmt3a*$^{R878H/+}$ double mutant mice 16 weeks

after pIpC induction of knock-in. (Error bars, mean ± SEM. Two-way ANOVA. * P <0.05) (B) Representative FACS gating scheme showing LSK and GMP populations in WT and *MxCreNpm1*$^{flox\text{-}cA/+}$ mice 16 weeks after pIpC injection. (C) Gene set enrichment analysis comparing genes induced by *Npm1c* in mouse GMPs (4 weeks post pIpC induction) to human *NPM1c* AML, (D) mouse stem cell signatures and (E) HSC markers (Table S3). (F) Scatter plot of Log2 fold changes in gene expression in *Npm1c* versus WT GMPs and (G) LSK cells, 4 weeks post pIpC treatment (n=3 mice per group). (H) qRT-PCR validation of changes in gene expression in WT, *MxCreNpm1*$^{flox\text{-}cA/+}$ single, and *MxCreNpm1*$^{flox\text{-}cA/+}$*Dnmt3a*$^{R878H/+}$ double mutant GMPs and (I) LSK cells, 4 weeks post pIpC treatment (n=3 mice per group).

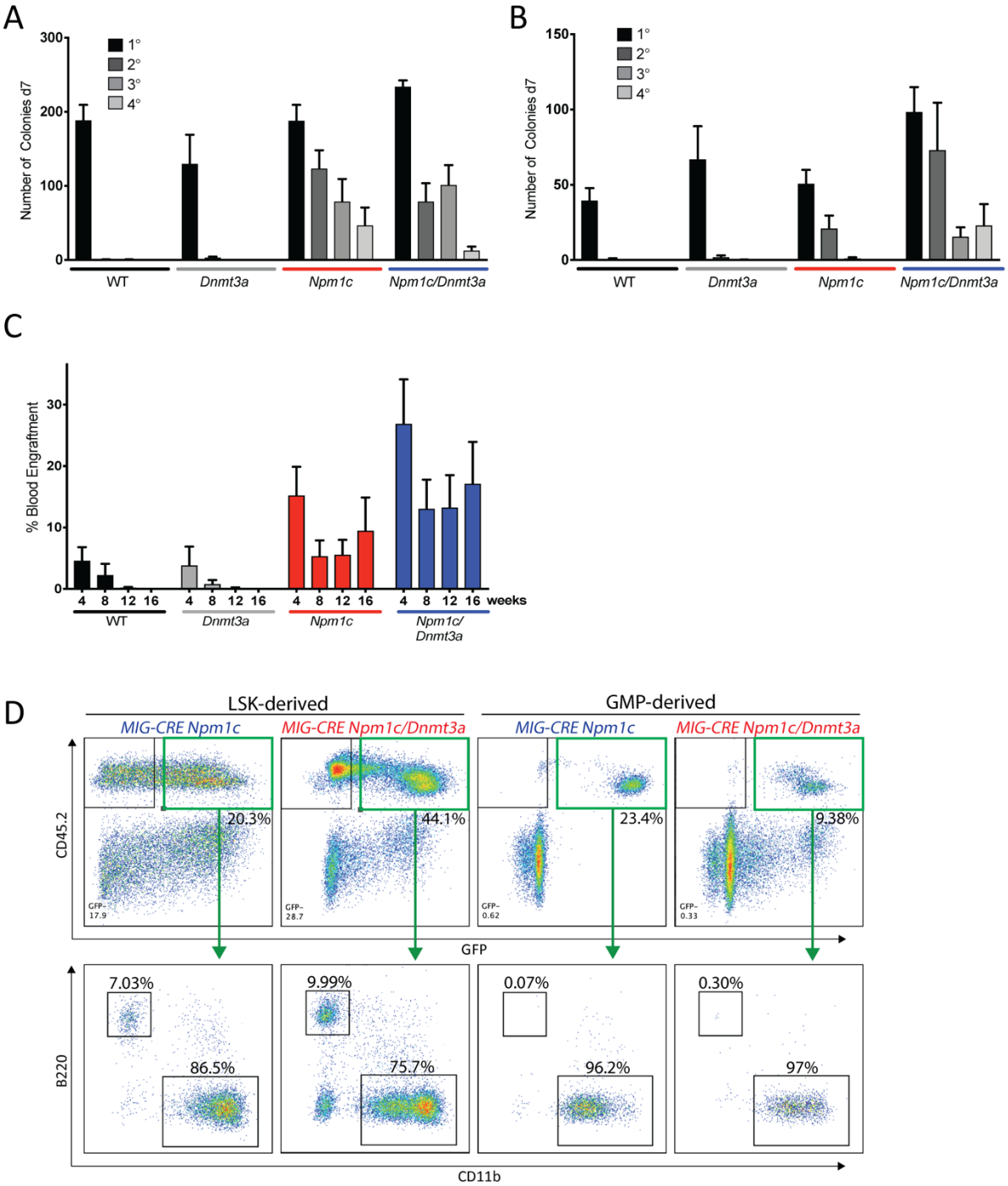

Fig. S2. *Npm1c* is sufficient to induce self-renewal properties in myeloid progenitor cells *in vitro* and *in vivo*.

(A) Colony forming assay of WT, *MxCreNpm1*$^{flox\text{-}cA/+}$ single, and *MxCreNpm1*$^{flox\text{-}cA/+}$*Dnmt3a*$^{R878H/+}$ double mutant GMPs sorted 4 weeks post pIpC induction of *Cre* excision *in vivo* (n≥6). (B) CFU replating assay using FACS sorted WT, *Dnmt3a*$^{R878H/+}$, *Npm1c*$^{flox\text{-}cA/+}$, and double mutant GMPs infected with retroviral *MIG-Cre in vitro* (n≥8 mice per group, error bars, mean ± SEM). (C) Summary of peripheral blood (%CD45.2) engraftment of *in vitro MIG-Cre* infected

WT and mutant GMPs, transplanted into lethally irradiated recipients (CD45.1). (D) Representative FACS plots of peripheral blood ($CD45.2^+$ and GFP^+) engraftment of *in vitro MIG-Cre* infected $Npm1^{flox\text{-}cA/+}Dnmt3a^{R878H/+}$ GMPs or LSK 7 months post-transplant analyzed for their expression of lymphoid (B220) and myeloid (CD11b) surface markers.

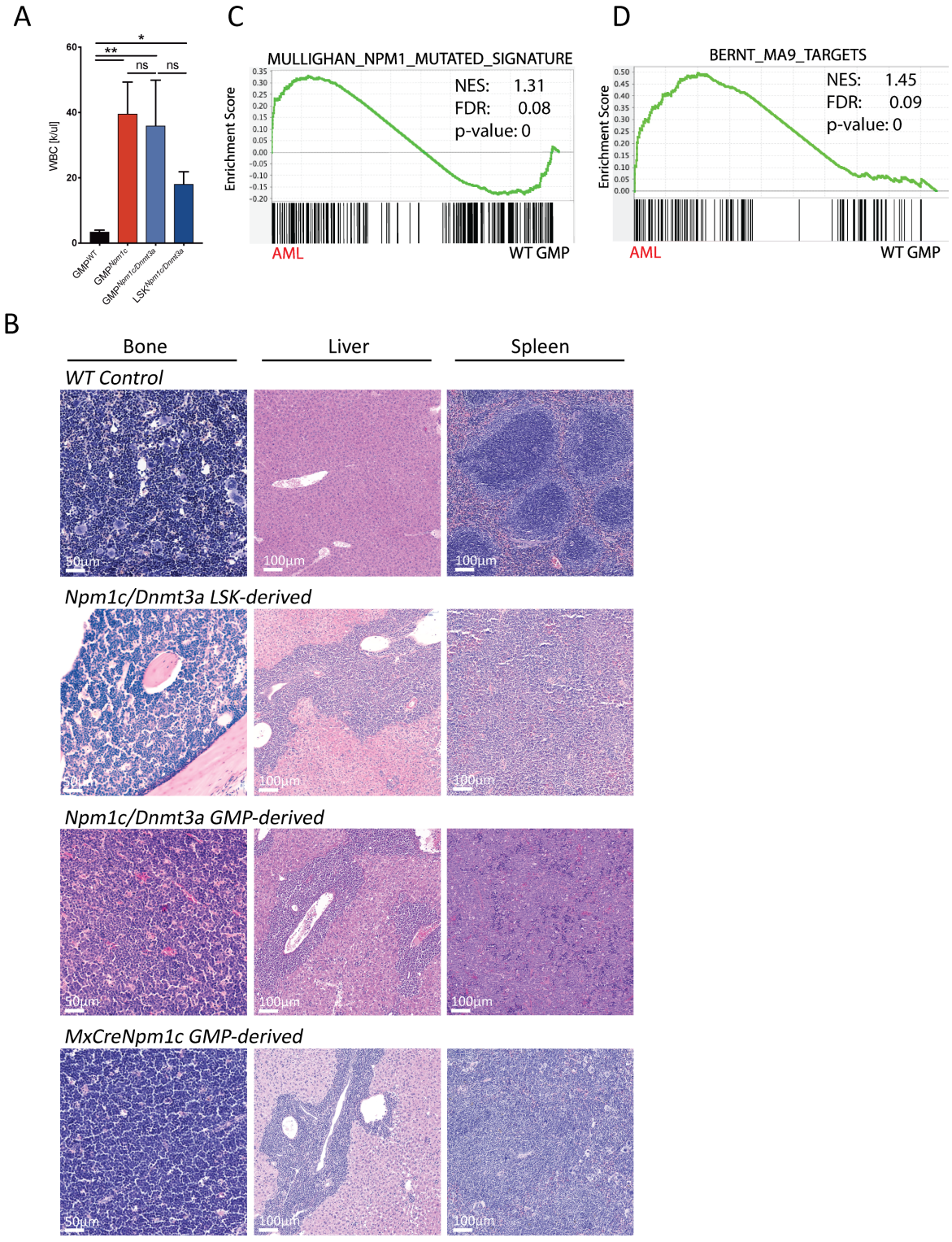

Fig. S3. Mouse *Npm1c*$^{+}$ AMLs can be derived from granulocyte and macrophage progenitors.

(A) Comparison of WBC counts of *MIG-CreNpm1*$^{flox\text{-}cA/+}$*Dnmt3a*$^{R878H/+}$ LT-GMP or LSK-derived and *MxCreNpm1c*$^{flox\text{-}cA/+}$ LT-GMP-derived leukemia bearing mice to WT control mice (n≥4 mice

per group). (B) Histological analysis of bone, spleen and liver sections of moribund mutant mice compared to WT control. (C) Gene set enrichment analysis comparing sorted mouse *MIG-CreNpm1*$^{flox\text{-}cA/+}$*Dnmt3a*$^{R878H/+}$ mutant AML cells to human *NPM1c*$^{+}$ AML and (D) *MLL-AF9* AML gene signatures (Table S3). ** P <0.01, *** P <0.001.

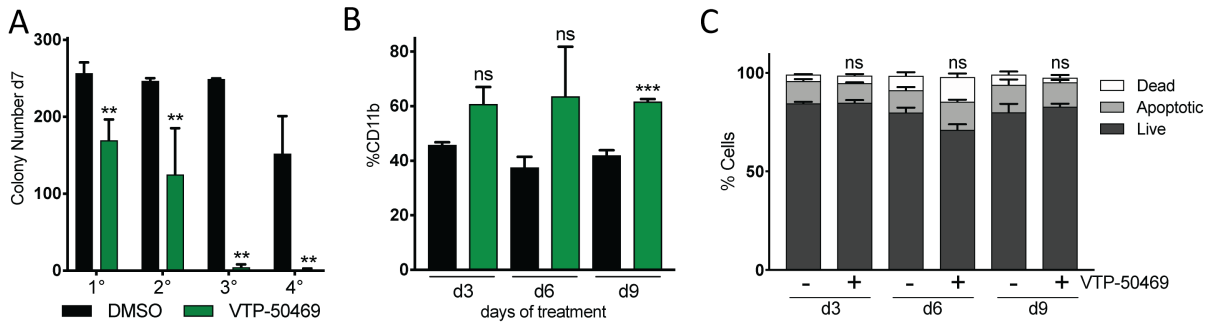

Fig. S4. *Npm1*$^{flox\text{-}cA/+}$ cell lines respond to VTP-50469 treatment by loss of self-renewal, upregulation of myeloid differentiation markers, and no increase in apoptosis.

(A) Colony forming assay of mouse *Npm1*$^{flox\text{-}cA/+}$ cell line serially replated every seven days in the presence of DMSO or 10 nM VTP-50469. Mean of three independent experiments. (B) FACS analysis of %CD11b expression and (C) Annexin V staining of mouse *Npm1*$^{flox\text{-}cA/+}$*Dnmt3a*$^{R878H/+}$ cell line (SIIIL12) treated with 10 nM VTP-50496 for 3, 6, and 9 days. Mean ± SEM. One-way ANOVA. ** P <0.01, *** P <0.001.

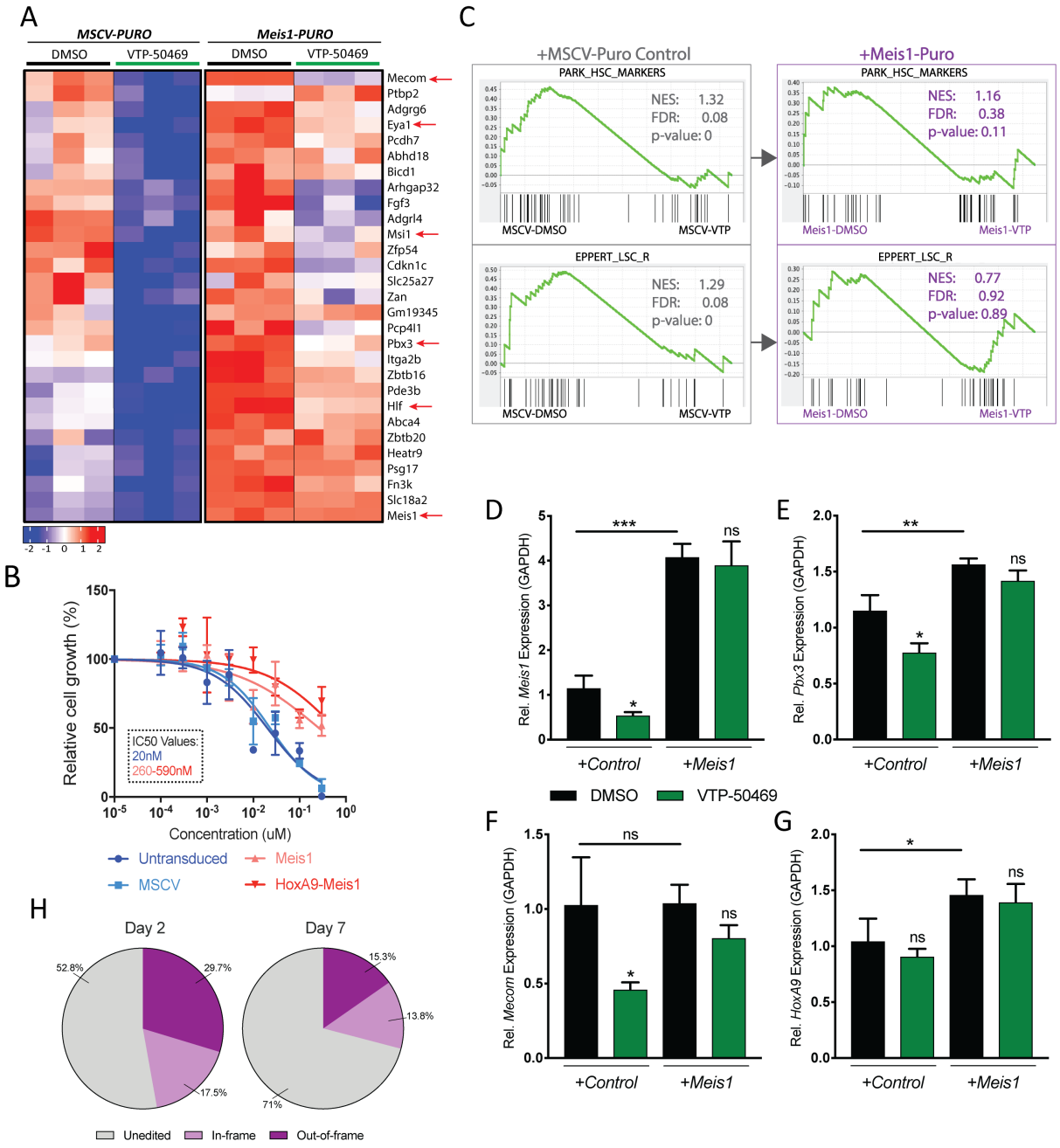

Fig. S5. *Meis1*-overexpression rescues parts of the leukemic stem cell program repressed by VTP-50469.

(A) Heatmap of genes repressed by VTP-50469 in MSCV-puro but rescued in Meis1-puro expressing mouse *NPM1*$^{flox\text{-}cA/+}$*Dnmt3a*$^{R878H/+}$ SIIIL12 cells. Red arrows indicate important stem cell genes (n=3). (B) VTP-50469 dose response curve of mouse *Npm1*$^{flox\text{-}cA/+}$*Dnmt3a*$^{R878H/+}$ cell line (SIIIL12) expressing *MSCV-IRES-puro* control (MSCV), *Meis1-IRES-puro (Meis1), or Meis1/HoxA9-IRES-hygro (HoxA9-Meis1)*. Representative of three independent experiments. (C) GSEA analysis assessing normal and leukemic stem cells signatures that are significantly repressed in *MSCV* control (left panel) but not in *Meis1* overexpressing (right panel) SIIIL12 cells

in response to 30 nM VTP-50469 treatment (day 3). (D) RT-PCR validation of *Meis1*, (E) *Pbx3,* (F) *Mecom*, (G) *HoxA9* expression in control (*MSCV-IRES-puro)* SIIIL12 versus *Meis1* overexpressing cells treated with 30 nM VTP-50469 (day 3). (H) Pie chart of percentage of CRISPR edits at the Meis1 locus that are in frame, out-of-frame, or unedited on day 1 and day 7 post electroporation with *sgMeis1* in SIIIL12 cells. One-way ANOVA. * P <0.05, ** P 0.01, *** P <0.001.

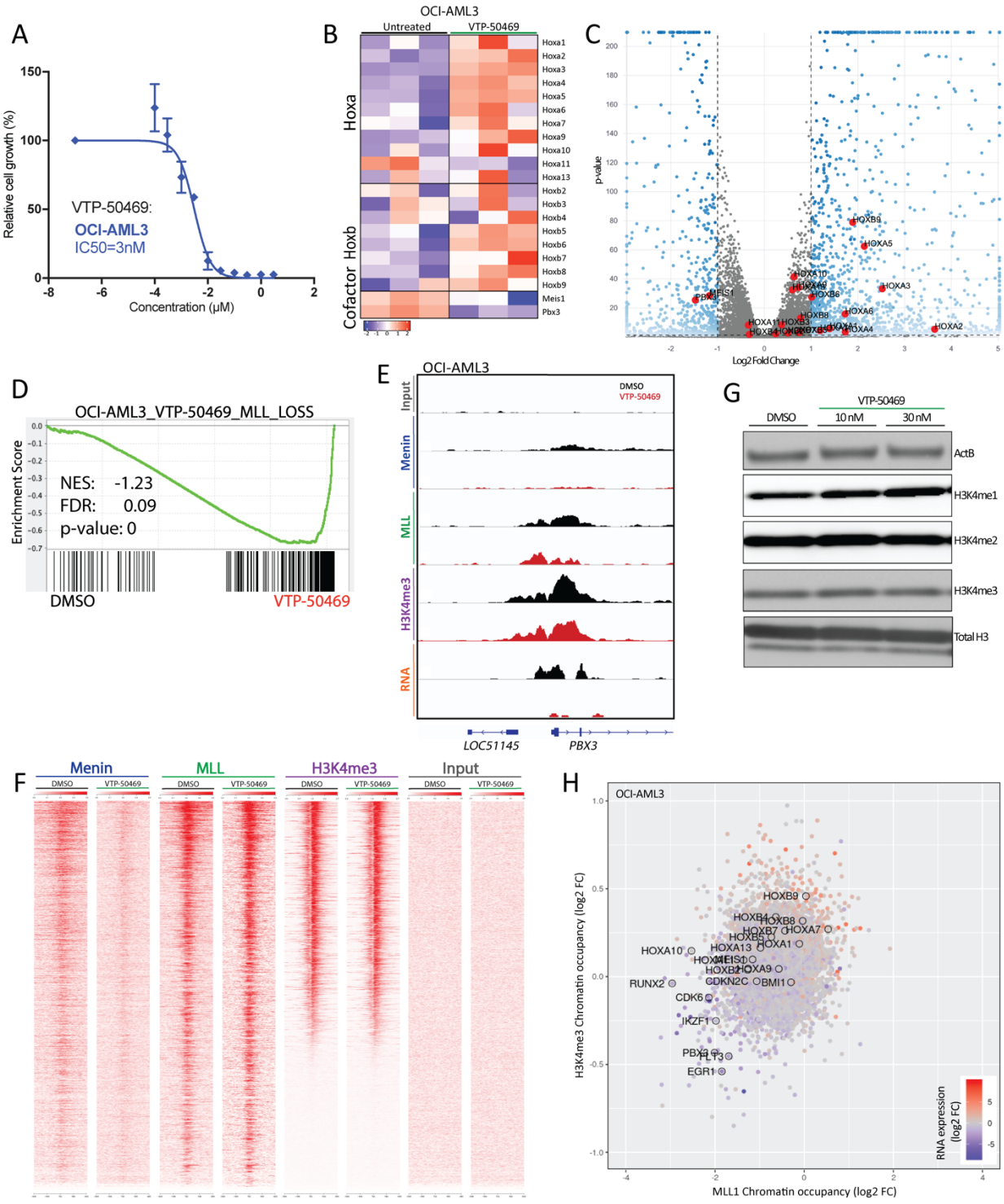

Fig. S6. Human cell line OCI-AML3 is sensitive to VTP-50469 treatment and shows repression of *MEIS1* and *PBX3* but not *HOXA/B* cluster genes.

(A) VTP-50469 dose response curve showing cell viability of OCI-AML3 cells and IC50 value on day 6. (B) Heatmap of *HOXA/B* cluster genes and co-factors *MEIS1* and *PBX3* (z-scores of

normalized counts) and (C) Scatterplot of RNAseq gene expression changes in OCI-AML3 cells (n=3, day 5, 330 nM VTP-50469). (D) GSEA analysis assessing loss of gene expression with top 200 genes that lose MLL in response to VTP-50469 treatment in OCI-AML3 cells. (E) ChIPseq density plots showing changes in chromatin occupancy of Menin and MLL as well as changes in mRNA expression in response to VTP-50469 treatment in OCI-AML3 cells at the TSS of *PBX3* (330 nM VTP-50469, ChIPseq day 4, RNAseq day 5). (F) Menin and MLL1 ChIP-seq data in OCI-AML3 shown as tornado plots of approximately 28,482 TSS+/-3kb showing global decrease in Menin but not MLL1 chromatin occupancy. (G) OCI-AML3 cells were treated with 10 nM or 30 nM VTP-50469 for 4 days and immunoblotted for b-Actin, H3K4me1/2/3 and total histone H3. (H) Scatter plot of Log2 fold changes in chromatin occupancy of MLL1 and H3K4me3 in OCI-AML3 cells treated with VTP-50469 for 4 days.

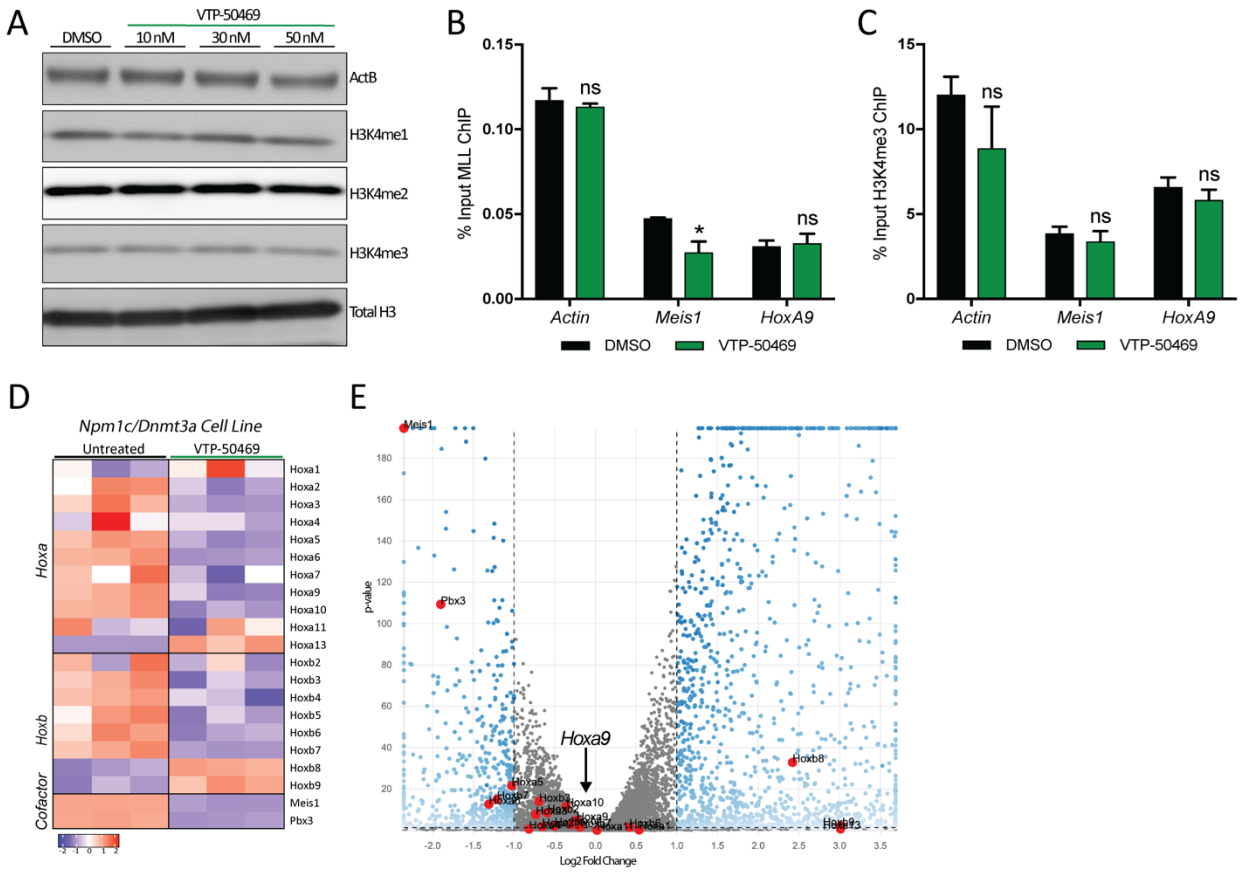

Fig. S7. Mouse *Npm1c/Dnmt3a* mouse cell line SIIIL12 shows reduced MLL1 binding at *Meis1* locus upon VTP-50469 treatment.

(A) Mouse SIIIL12 cells were treated with 10, 30 or 50 nM VTP-50469 for 4 days and immunoblotted for b-Actin, H3K4me1/2/3 and total histone H3. (B) MLL1 chromatin occupancy determined by ChIP-qPCR analysis of mouse SIIIL12 cells treated with 100 nM VTP-5046 for 4 days. (C) H3K4me3 histone mark quantified by ChIP-qPCR analysis of mouse SIIIL12 cells treated with VTP-5046 for 4 days. One-way ANOVA. * P <0.05. (D) Summary of RNAseq gene expression analysis (z-scores of normalized counts) of *Hoxa/b* cluster and co-factors *Meis1* and *Pbx3* in mouse *Npm1c/Dnmt3a* mutant SIIIL12 cells treated with 100 nM VTP-5046 for 4 days. (E) Scatter plot of Log2 fold changes in gene expression in SIIIL12 cells treated with 100 nM VTP-5046 for 4 days (n=3).

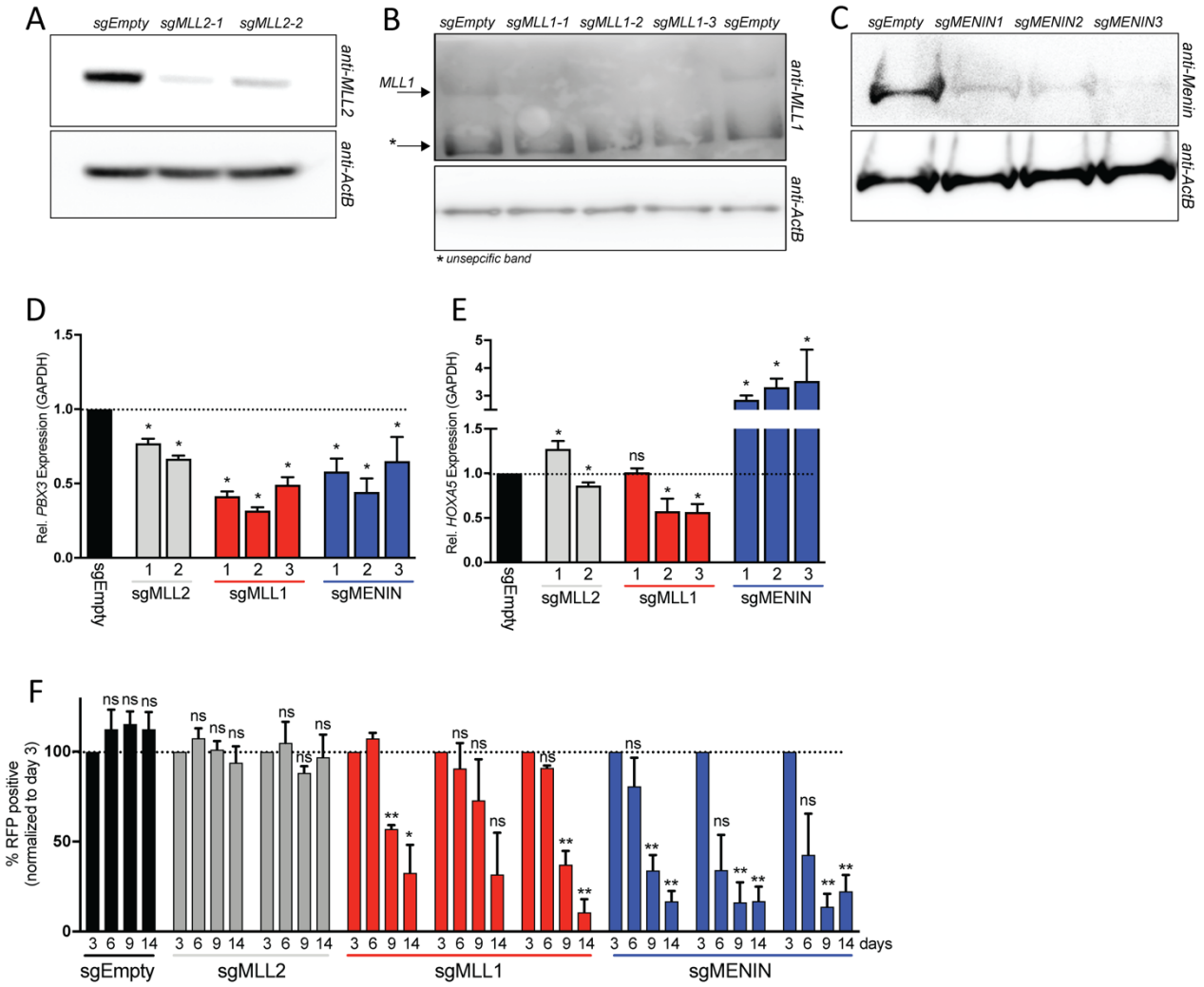

Fig. S8. Knock-out of *MLL1*, but not *MLL2* leads to reduction in *HOXA/B* expression as well as *MEIS1* and *PBX3* in OCI-AML3 cells.

(A) Immunoblot validation of CRISPR Cas9 mediated knock-out of *MLL2, (B) MLL1,* and (C) *Menin* in OCI-AML3 cells day 5 post transduction with sgRNA lentivirus using three independent sgRNAs. (D) Gene expression analysis of *PBX3* and (E) *HOXA5,* 5 days after sg*MLL1*, sg*MLL2,* and *sgMenin* transduction assessed by qRT-PCR. Mean of three independent experiments. (F) Negative selection competition assay plotting %RFP$^+$ (sgRNA$^+$) cells at indicated time-points after lentiviral transduction normalized to %RFP$^+$ cells on day 3. Mean of three independent experiments ± SEM.* P <0.05, ** P <0.01.

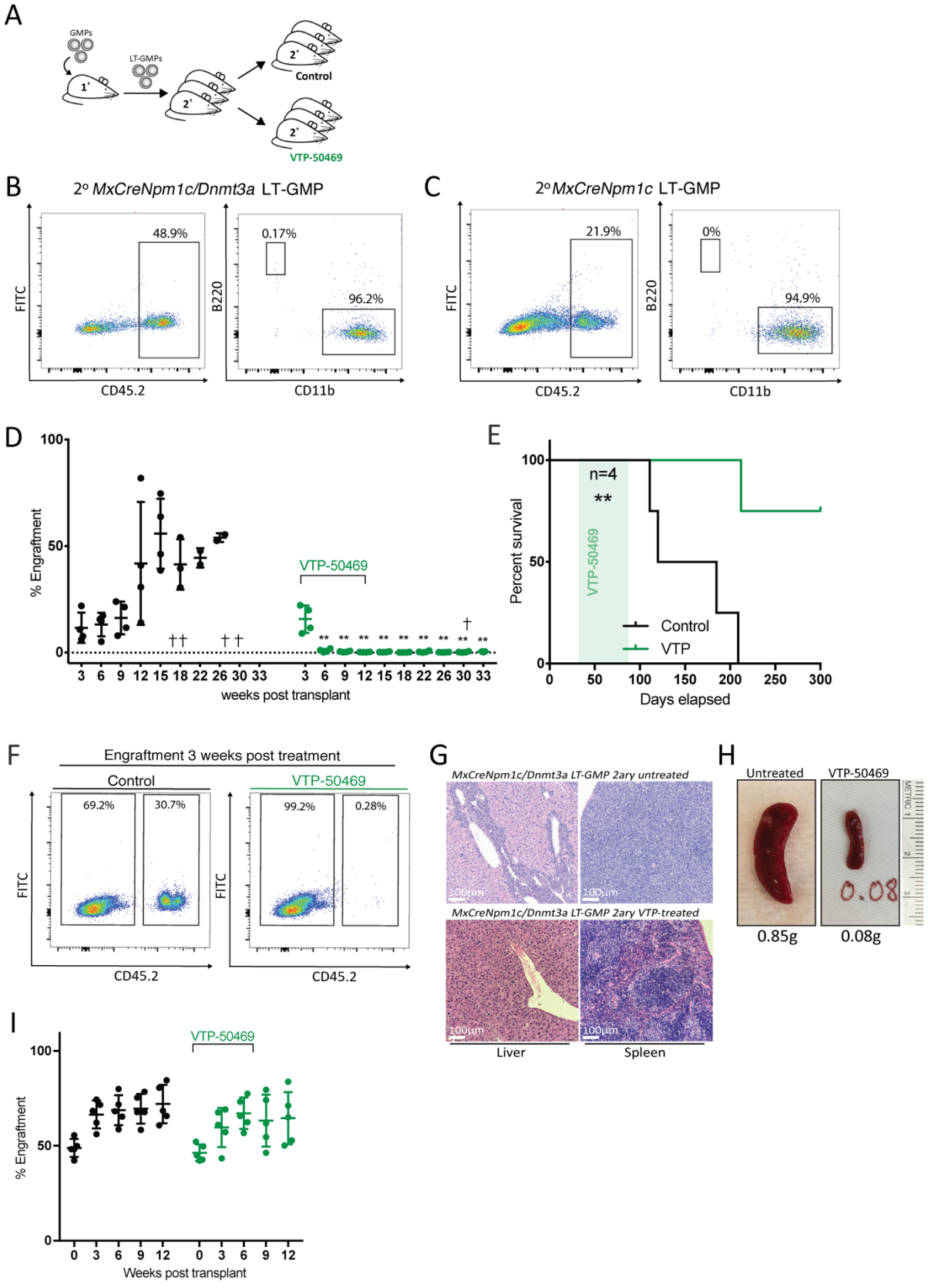
A
GMPs
LT-GMPs
1°
2°
2°
Control
2°
VTP-50469
B
2° MxCreNpm1c/Dnmt3a LT-GMP
48.9%
0.17%
96.2%
FITC
B220
CD45.2
CD11b
C
2° MxCreNpm1c LT-GMP
21.9%
0%
94.9%
FITC
B220
CD45.2
CD11b
D
% Engraftment
100
50
0
VTP-50469
3 6 9 12 15 18 22 26 30 33 3 6 9 12 15 18 22 26 30 33
weeks post transplant
E
Percent survival
100
50
0
n=4
**
VTP-50469
Control
VTP
0 50 100 150 200 250 300
Days elapsed
F
Engraftment 3 weeks post treatment
Control
VTP-50469
69.2%
30.7%
99.2%
0.28%
FITC
CD45.2
G
MxCreNpm1c/Dnmt3a LT-GMP 2ary untreated
MxCreNpm1c/Dnmt3a LT-GMP 2ary VTP-treated
100µm
Liver
Spleen
H
Untreated
VTP-50469
0.08
0.85g
0.08g
I
VTP-50469
% Engraftment
100
50
0
0 3 6 9 12 0 3 6 9 12
Weeks post transplant

Fig. S9. Pre-leukemic LT-GMPs are highly sensitive to Menin-MLL inhibition and can be eradicated by *in vivo* VTP-50469 treatment.

(A) Experimental overview: Mice were transplanted with long-term engrafted GMPs (LT-GMPs), secondary engraftment was confirmed after 3 weeks, and mice were separated into control and 0.1% VTP-50469 chow treatment groups. (B) Representative FACS plots confirming secondary *MxCreNpm1*$^{flox\text{-}cA/+}$*Dnmt3a*$^{R878H/+}$ double and (C) *MxCreNpm1*$^{flox\text{-}cA/+}$ single mutant LT-GMP engraftment 3 weeks after transplant. (D) Percent peripheral blood CD45.2 engraftment of *MxCreNpm1*$^{flox\text{-}cA/+}$ LT-GMP 2ary transplants treated with control or 0.1% VTP-50469 spiked chow for 9 weeks (n=4 mice per group). (E) Kaplan-Meyer survival analysis showing significantly increased survival of *MxCreNpm1*$^{flox\text{-}cA/+}$ LT-GMP secondary recipient mice dosed with VTP-50469. (F) Representative FACS plot comparing CD45.2 engraftment of LT-GMP 2^{ary} recipients after 3 weeks of control or VTP-50469 treatment. (G) Histological analysis of liver and spleen of *MxCreNpm1*$^{flox\text{-}cA/+}$*Dnmt3a*$^{R878H/+}$ LT-GMP secondary recipient mice treated with control or VTP-50469 spiked chow (9 weeks). (H) Representative spleen image of an untreated versus a VTP-50469 treated *MxCreNpm1*$^{flox\text{-}cA/+}$*Dnmt3a*$^{R878H/+}$ LT-GMP secondary recipient. (I) Percent peripheral blood CD45.2 engraftment of secondary transplants of FACS sorted WT HSCs (LSKCD150^{+}CD48$^{-;}$ n=5 mice per group).

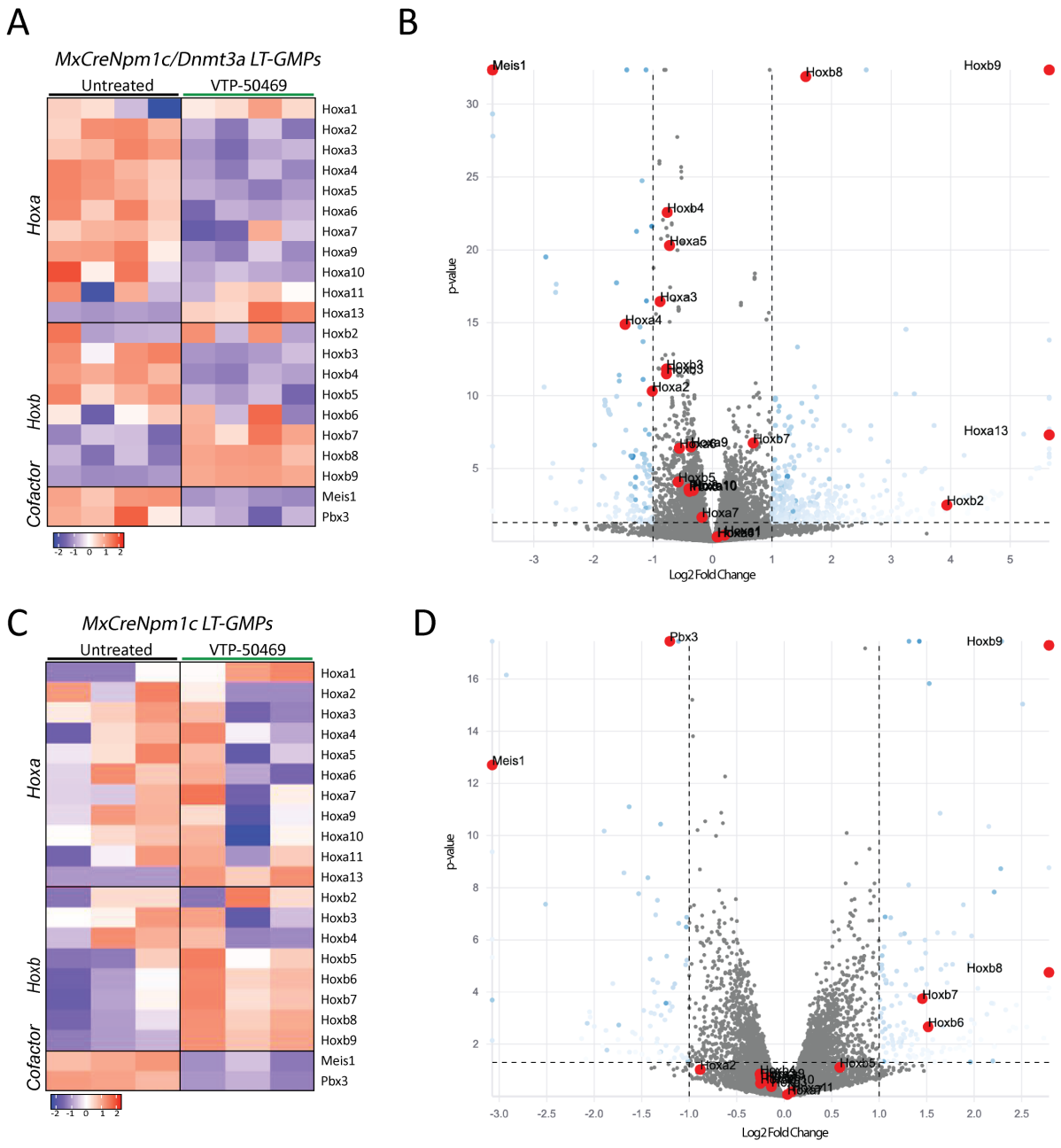

Fig. S10. *In vivo* VTP-50469 treated mouse LT-GMPs strongly repress *Meis1* and *Pbx3* expression with varying effects on *Hoxa/b* expression.

(A) Heatmap of RNAseq gene expression (z-scores of normalized counts) of *HoxA/B* cluster genes and co-factors *Meis1* and *Pbx3* of *MxCreNpm1*$^{flox\text{-}cA/+}$*Dnmt3a*$^{R878H/+}$ LT-GMPs treated with VTP-50469 in vivo for 5 days. (B) Scatter plot of Log2 fold changes in gene expression of *MxCreNpm1*$^{flox\text{-}cA/+}$*Dnmt3a*$^{R878H/+}$ LT-GMPs treated with VTP-50469 in vivo for 5 days. (n=4 mice) (C) Heatmap of RNAseq gene expression (z-scores of normalized counts) of *HoxA/B* cluster genes and co-factors *Meis1* and *Pbx3* of *MxCreNpm1*$^{flox\text{-}cA/+}$ LT-GMPs treated with VTP-50469 in

vivo for 5 days. (D) Scatter plot of Log2 fold changes in gene expression of *MxCreNpm1*$^{flox\text{-}cA/+}$ LT-GMPs treated with VTP-50469 in vivo for 5 days. (n=3 mice).

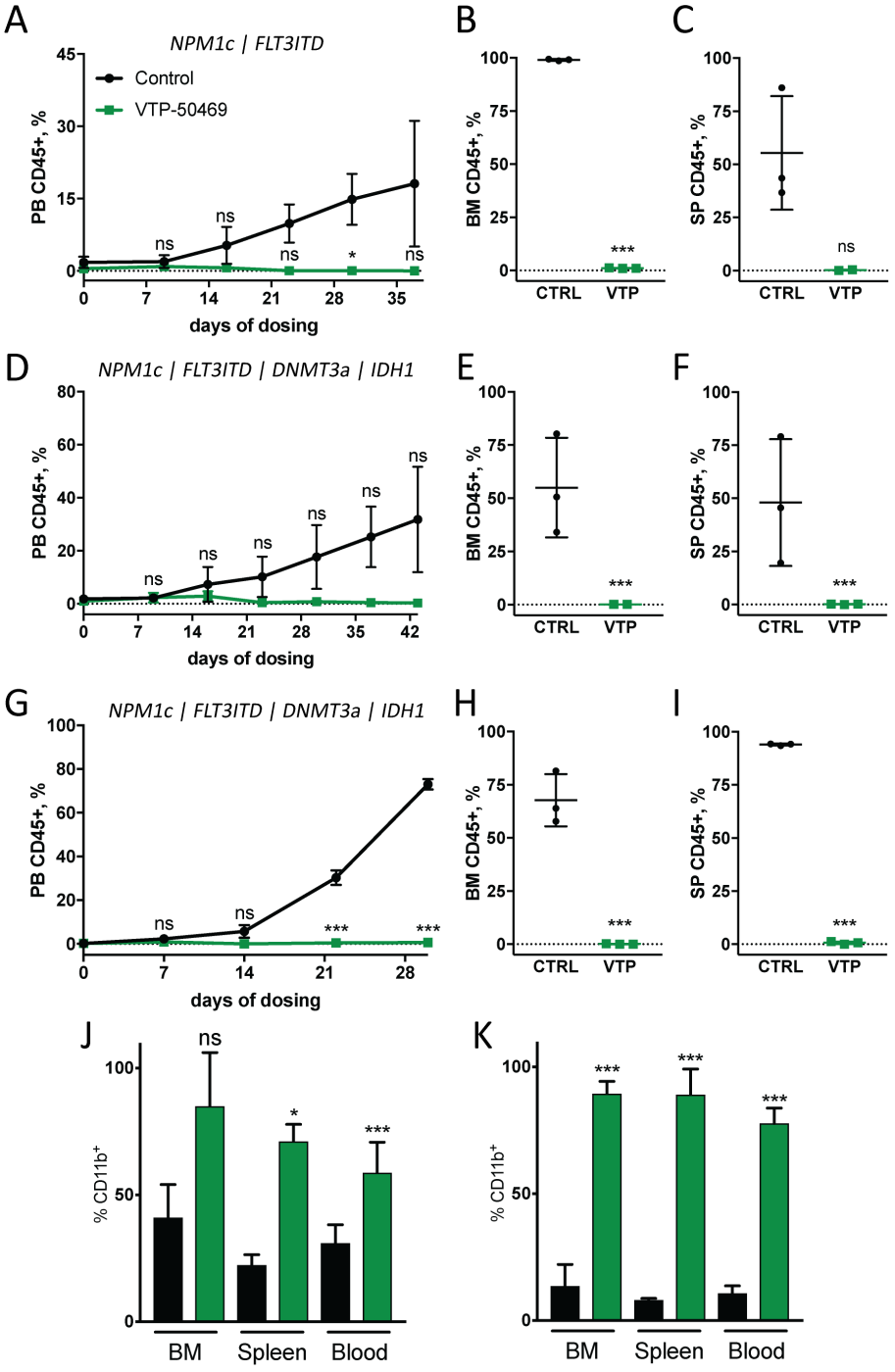

Fig. S11. VTP-50469 suppresses growth and induces differentiation in human *NPM1c* mutant AML cells in PDX models.

(A) Percent human CD45 (hCD45) engraftment of *NPM1c/FLT3ITD* mutant AML cells (Patient #2, table S4) in peripheral blood of NOG mice over time and in (B) bone marrow and (C) spleen

at end point (day 37 of treatment, n=3 mice per group). (D) Percent hCD45 engraftment of *NPM1c/FLT3ITD/DNMT3A/IDH1* mutant AML cells (Patient #3, table S4) in peripheral blood of NOG mice over time and (E) bone marrow and (F) spleen at end point (day 43; n=3 mice pre group). (G) Percent hCD45 engraftment of *NPM1c/FLT3ITD/DNMT3A/IDH1* mutant AML cells (Patient #4, table S4) in peripheral blood of NOG mice over time and (H) bone marrow and (I) spleen at end point (day 30, n=3). (J) Summary of BM, spleen and peripheral blood %$CD11b^+$ expression on $hCD45^+$ cells after *in vivo* VTP treatment of PDX sample #3 and (K) PDX sample #4 at endpoint (n=3 mice per group). Student's t-test. *$P < 0.05$, **$P < 0.01$, ** P <0.01, *** P <0.001.

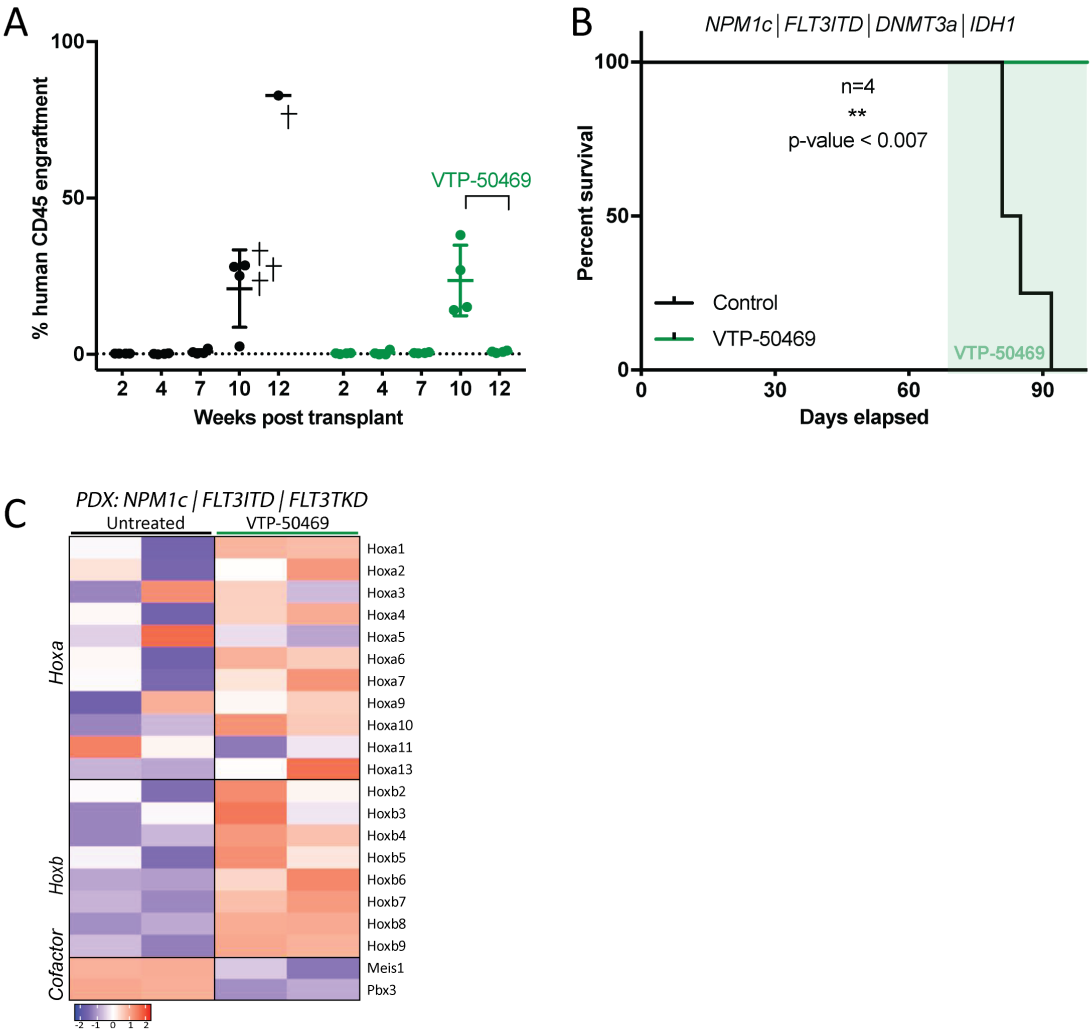

Fig. S12. VTP-50469 treatment of *NPM1c* mutated human PDX models shows rapid reduction of peripheral blood engraftment and enhanced survival.

(A) Human CD45 engraftment (%) in peripheral of control or VTP-50469 treated patient derived *NPM1c/FLT3ITD/DNMT3a/IDH1* mutant AML cells (Patient sample # 4, see table S5) in NOG mice (n=4 mice per group). (B) Kaplan-Meyer survival curve of *NPM1c/FLT3ITD/DNMT3A/IDH1* mutant AML PDX model (Patient # 4) receiving control or VTP-50469 spiked chow starting on day 70 post-transplant. (C) Summary of RNAseq gene expression analysis (z-scores of normalized counts) of *HOXA/B* cluster and co-factors *MEIS1* and *PBX3* in duplicate PDX samples harvested 10 days post VTP-50469 treatment *in vivo* (Patient #1, table S5).

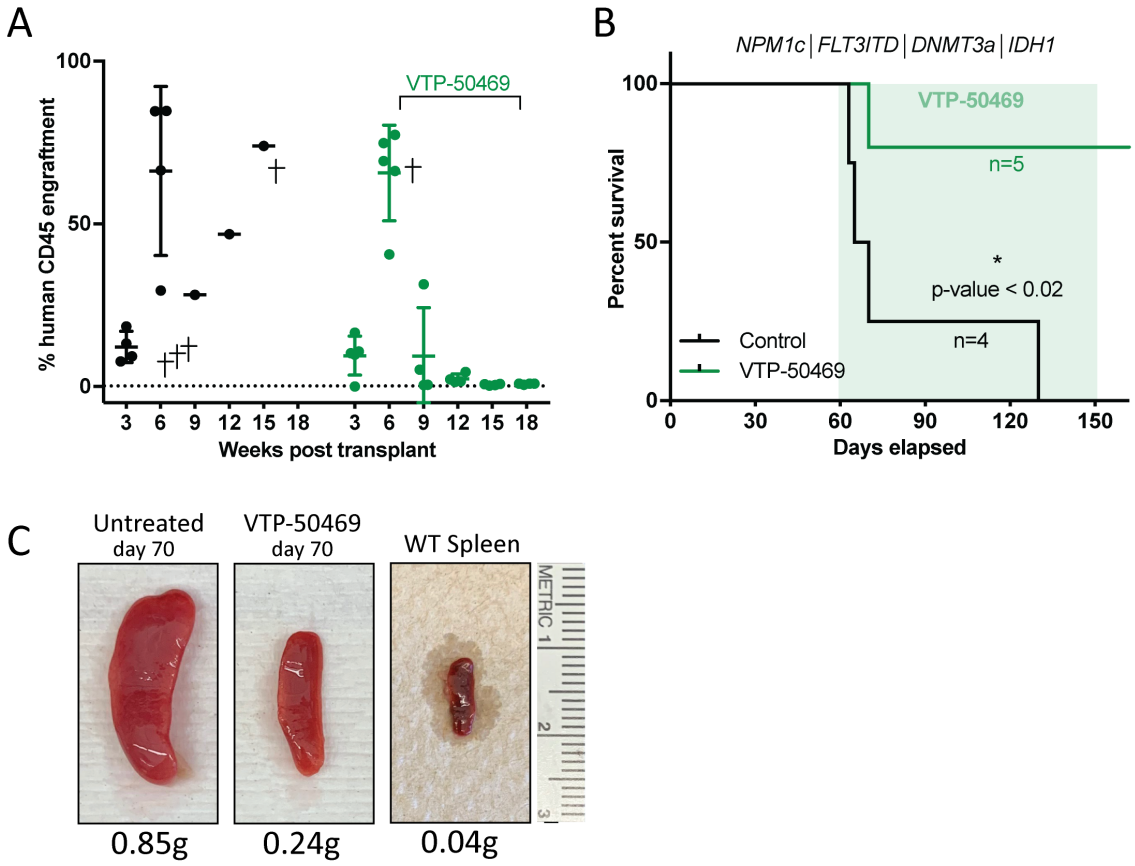

Fig. S13. VTP-50469 effectively eradicates highly engrafted human *NPM1c*$^{+}$ AML cells in PDX mice.

(A) Human CD45 engraftment (%) in peripheral of control or VTP-50469 treated patient derived *NPM1c/FLT3ITD/DNMT3A/IDH1* mutant AML cells (Patient sample # 4, table S5) in NOG mice (n=4 control and n=5 VTP-50469 treated mice per group). (B) Kaplan-Meyer survival curve of highly engrafted (average >50% hCD45) *NPM1c/FLT3ITD/DNMT3A/IDH1* mutant AML PDX model receiving control or VTP-50469 spiked chow for 90 days. (C) Spleen images of WT NOG control and moribund *NPM1c/FLT3ITD/DNMT3A/IDH1* mutant AML PDX mice sacrificed on day 70 post-transplant showing reduced spleen size in VTP-50469 treated mouse 10 days post treatment.